

Contribution from the Departments of Chemistry, University of Oregon, Eugene, Oregon 97403, and Columbia University, New York, New York 10027

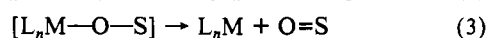
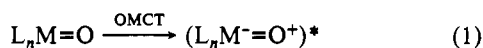
Descriptive Photochemistry and Electronic Structure of the Cp_2MoO and $(MeCp)_2MoO$ Complexes ($Cp = \eta^5-C_5H_5$; $MeCp = \eta^5-CH_3C_5H_4$)

Ned D. Silavve,^{1,2} Mitchell R. M. Bruce,^{2,3} Cecelia E. Philbin,^{1,2} and David R. Tyler*^{1,2}

Received April 15, 1988

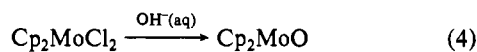
The photochemistry of the Cp_2MoO and $(MeCp)_2MoO$ complexes was studied because these complexes are potential photochemically activated oxygenating agents. Irradiation of these complexes in deoxygenated solutions initially forms Cp_2Mo (or $(MeCp)_2Mo$) and O_2 : $2Cp_2MoO \xrightarrow{h\nu} 2Cp_2Mo + O_2$. The products that subsequently form arise from the reaction of the photogenerated O_2 with Cp_2MoO and Cp_2Mo . Thus, Cp_2MoO reacted with O_2 to give $[Cp_2Mo(MoO_4)]_2$. Cp_2Mo dimerized to give $C_{20}H_{18}Mo_2$, and this species subsequently reacted with O_2 to give an unidentified oxide (complex A). In the presence of ligands, Cp_2Mo was captured to give Cp_2MoL -type products ($L = CO, PR_3, olefin$). In the presence of SEt_2 , $CpMo(H)Et$ formed. In no case, except PPh_3 , was oxygen atom transfer to any substrate (olefin, phosphine, amine, sulfide) observed. In the case of PPh_3 , $OPPh_3$ probably formed by reaction of O_2 with PPh_3 . Photochemical oxygen atom transfer from Cp_2MoO to the substrates failed because Cp_2Mo is a better oxygen atom acceptor than the substrates. The electronic structure of the Cp_2MoO complex was investigated by using the self-consistent-field-X α -scattered-wave (SCF-X α -SW) molecular orbital method. The calculation showed that the Mo-O bond is best described as being intermediate between a double and a triple bond. This conclusion is consistent with X-ray diffraction and infrared spectroscopic results [$d(Mo-O) = 1.721(2) \text{ \AA}$; $\nu(Mo-O) = 827 \text{ cm}^{-1}$ for $(MeCp)_2MoO$]. The calculation predicts a d-d excited state at lowest energy, with $O \rightarrow Mo$ and $Cp \rightarrow Mo$ charge-transfer states at higher energy. The photochemistry was independent of wavelength; the lowest energy d-d excited state ($13a_1 \rightarrow 8b_1$; $^1A_1 \rightarrow ^1B_1$) is apparently the reacting state.

We are studying the photochemistry of organometallic oxide complexes because these species are potentially useful as photochemically activated oxygenating agents. One of many possible photochemical schemes for the oxygenation of a substrate, S, by a metal oxide is shown as follows:



The key to oxygen atom transfer in this scheme is the oxygen-to-metal charge-transfer excited state (OMCT); as a consequence of the charge transfer, the oxygen atom becomes electrophilic and is therefore susceptible to nucleophilic attack by the substrate (eq 2).

We began our photochemical study of organometallic oxide complexes with the Cp_2MoO and $(MeCp)_2MoO$ complexes. These complexes were first prepared by Green and co-workers by stirring a suspension of Cp_2MoCl_2 in aqueous base:⁴



Green's mass spectral data suggested a monomeric structure, a result later confirmed when we obtained the crystal structure of $(MeCp)_2MoO$.⁵ In this paper we report the results of an SCF-X α -MO calculation on Cp_2MoO (used to identify the charge-transfer absorption bands), we discuss the descriptive photochemistry of the Cp_2MoO complex, and we discuss the oxygen atom transfer reactions of this complex. A subsequent paper will deal with the mechanistic points raised herein.

Experimental Section

All manipulations and measurements were carried out under an inert atmosphere by using Schlenk techniques, vacuum-line techniques, or a Vacuum Atmospheres Co. drybox.

General Irradiation Procedure. Photolyses were generally carried out in sealed NMR tubes or in Schlenk flasks by using a 200-W high-pressure mercury arc lamp. Typically, 20–30-mg samples of Cp_2MoO were irradiated for several hours; specific times are given under Results where appropriate. In general, the irradiations produced a color change in the solution accompanied by the formation of a brown precipitate. Following irradiation, the precipitate was separated from the solution by filtration. Spectroscopic analysis of the filtrate and the precipitate then followed. The brown precipitate always contained $[Cp_2Mo(MoO_4)]_2$ and a second

component, complex A. (Complex A is discussed further below.) The Cp_2MoO complexes not only are quite air-sensitive but also decompose in oxygen-free solution, sometimes very slowly and other times more rapidly depending on the nature of the medium. The products formed in the dark reactions are similar to those formed in the photochemical reactions. Because of the thermal component, the photochemical reactions were always compared to a dark reaction as a control. The thermal reactions could be prevented by carrying out the photochemical reactions at 0 °C.

Reagents. Acetone, acetonitrile, benzene, diethyl sulfide, dimethyl sulfide, dichloromethane, 1,2-dimethoxyethane, 1,6-lutidine, methanol, 2-picoline, 4-picoline, pyridine, 2-propanol, 1-pentene, propylene carbonate, tetrahydrofuran, toluene, and tetrahydrothiophene were purified according to standard methods.⁶ 1-Methylimidazole was dried over NaOH by refluxing for 6 h, distilled, and kept over freshly activated 4-Å molecular sieves. Acetone- d_6 , benzene- d_6 , dimethyl- d_6 sulfoxide (DMSO- d_6), *N*-methylmorpholine *N*-oxide, and pentamethylene sulfide were obtained from Aldrich and used as received. Propylene oxide (Fisher Baker Analyzed Reagent grade) was used without further purification.

Triphenylphosphine (Aldrich) was recrystallized from hot 1:1 benzene/ethanol and then dried under vacuum at 50 °C. Imidazole (Aldrich) was recrystallized from benzene and then dried under vacuum. 1,3-Dithiane, molybdenum pentachloride (98%), pyrazole (98%), 4-picoline *N*-oxide (98%), pyridine *N*-oxide, quinuclidine, trimethylamine *N*-oxide dihydrate, and tungsten hexachloride were used as received from Aldrich.

Instrumentation. ¹H NMR spectra were obtained on a Varian XL-200 or General Electric QE-300 spectrometer. Infrared spectra were obtained on a Perkin-Elmer 289, Perkin-Elmer 983, or Nicolet DX FTIR spectrophotometer. Solution infrared spectra in the range 1000–4000 cm^{-1} were run by using CaF_2 cells with a path length of 0.05 mm. Sodium chloride solution cells and Nujol mulls on sodium chloride plates were used to run spectra in the 600–4000- cm^{-1} range.

Electronic spectra were run on a Cary 17, Beckman DU-7, or HP8452A spectrophotometer. Spectra were obtained in solution and Nujol mulls by using quartz cuvettes. Low-temperature electronic spectra were obtained by using a special quartz Dewar flask into which was fitted a long-stemmed quartz cuvette surrounded with an appropriate coolant. The Dewar flask had polished windows that could be aligned with those of the cuvette.

- (1) University of Oregon.
- (2) Columbia University.
- (3) Present address: Department of Chemistry, University of Maine, Orono, ME 04469.
- (4) Green, M. L. H.; Lynch, A. H.; Swanwick, M. G. *J. Chem. Soc., Dalton Trans.* 1972, 1445–1447.
- (5) Silavve, N. D.; Chiang, M. Y.; Tyler, D. R. *Inorg. Chem.* 1985, 24, 4219–4221.
- (6) Perrin, D. D.; Armarego, W. L. F.; Perrin, D. R. *Purification of Laboratory Chemicals*, 2nd ed.; Pergamon: New York, 1980.

* To whom correspondence should be addressed at the University of Oregon.

Table I. Selected Spectroscopic Data

complex	$^1\text{H NMR}, \delta$	IR, cm^{-1}
$\text{C}_{20}\text{H}_{18}\text{Mo}_2^a$	3.0 (multiplet, 2 H), 4.01 (multiplet, 2 H), 4.54 (s, 10 H), 4.84 (multiplet, 2 H), 5.40 (multiplet, 2 H)	911 (s), 881 (m), 850 (w)
$[\text{Cp}_2\text{Mo}(\text{MoO}_4)]_2^b$		3080 (m), 1605 (m), 1070 (s), 1018 (s), 953 (s), 915 (m), 885 (s), 839 (m), 812 (w)
A^c	6.43 (multiplet, 2 H), 5.09 (s, 10 H), 4.97 (multiplet, 2 H), 4.13 (multiplet, 2 H), 3.70 (multiplet, 2 H)	800 [$\nu(\text{Mo}=\text{O})$]
Cp_2MoO^d	5.11 (s)	3067 (m), 1368 (w), 1486 (w), 1023 (w), 847 (s), 827 (vs) [$\nu(\text{Mo}=\text{O})$], 818 (s) ^b
$(\text{MeCp})_2\text{MoO}$	1.67 (s, Me), 4.20 (t, Cp, 2.2 Hz), 5.90 (t, Cp, 2.2 Hz), ^d 1.60 (s, Me), 4.81 (t, Cp, 2.3 Hz), 6.10 (t, Cp, 2.1 Hz) ^e	$\nu(\text{C}=\text{O}): 1907,^e 1915^f$
Cp_2MoCO		
$\text{Cp}_2\text{Mo}(\text{H})\text{SEt}^d$	-7.37 (s, Mo-H), 1.43 (t, $-\text{CH}_3$, 7.3 Hz), 2.52 (q, $-\text{SCH}_2-$, 6.2 Hz), 4.44 (d, Cp, 1.4 Hz)	
$\text{Cp}_2\text{Mo}(\text{H})\text{SMe}^d$	-7.35 (s, MoH), 2.02 (s, CH_3), 4.45 (d, Cp, 1.4 Hz)	

^a Acetone- d_6 . ^b Nujol Mull. ^c DMSO- d_6 . ^d Benzene- d_6 . ^e Pyridine. ^f Benzene.

Mass spectra were obtained with a Nermag R10-10 Quadrupole or the HP782/H712 instruments. Elemental analyses were done by Galbraith Laboratories.

Quantum Yield Measurements. A weighed amount of sample was dissolved in an appropriate solvent, and the resulting solution was split into two portions, with one serving as a dark-reaction control. The absorbance of each solution was recorded before irradiation and then again after fixed intervals of irradiation. The absorbance of the irradiated solution was corrected for any thermal reaction by subtracting from it the reading for the control solution. The change in absorbance was then used for the calculation of the quantum yield.

Although solutions in 1-methylimidazole and *n*-butylamine remained homogeneous throughout photolysis, those in pyridine or benzene or those containing some 1-methylimidazole or *n*-butylamine produced insoluble products. Filtration or centrifugation after photolysis was therefore necessary before taking absorbance readings with the latter solvents. These manipulations were carried out under an inert atmosphere.

Corning glass filters were used for wavelength selection. Lamp intensities were measured by using Aberchrome 540 actinometry.⁷ The amount of light absorbed by the actinometer or sample was corrected by appropriate expressions whenever the absorbance at the wavelength being used for irradiation was less than 2.⁸

Materials. The Cp_2MoH_2 ,⁹ $(\text{MeCp})_2\text{MoH}_2$,¹⁰ Cp_2MoO ,⁴ and $(\text{MeCp})_2\text{MoO}$ ⁵ complexes were prepared by literature methods.

A Method for the Purification of $(\text{RC}_2\text{H}_4)_2\text{MoO}$ ($\text{R} = \text{H}, \text{CH}_3$). The purification of the metallocene oxides after extraction with benzene was accomplished by chromatographing the complexes through a column of a specially prepared alkaline alumina. The metallocene oxides and their corresponding dihydrides decompose on normal basic, neutral, or acidic alumina. To prevent decomposition, the following procedure should be followed. Either basic, neutral, or acidic alumina may be used. The alumina is added to a saturated solution of NaOH in EtOH to form a slurry. Following filtration through a frit, the alumina is dried at 140–160 °C for 12 h and then cooled in an inert atmosphere.

The chromatography column is made in an inert atmosphere in a nonpolar solvent such as hexane. The sample is introduced onto the top of the column as a benzene solution. Elution with a hexane/benzene solvent mixture (1/4) gives Cp_2MoH_2 (as a yellow or brown solution). Subsequent elution with a benzene/THF solvent mixture (1/1) gives a green solution of the oxide. The use of neat THF accelerates the elution rate; however, the product is sometimes contaminated with impurities when this is done. Evaporation of the solvent yields emerald green Cp_2MoO . For a purer oxide, the product may be recrystallized from heptane/benzene (or THF).

Irradiation of Cp_2MoO and Olefins or Acetylenes. A mixture of Cp_2MoO (40 mg, 0.16 mmol) and 1-hexene (52 mg, 0.62 mmol) in benzene- d_6 was irradiated ($\lambda > 240$ or 340 nm) for 8 h. The color of the solution changed from green to brown, and a brown precipitate was deposited. The $^1\text{H NMR}$ spectrum of the solution showed the presence of $\text{C}_{20}\text{H}_{18}\text{Mo}_2$ (30%) and a small amount of unreacted Cp_2MoO (4%).

There were also weak resonances at δ 3.99 (s) and 4.04 (s) attributable to Cp_2Mo (1-hexene).¹¹ A control dark reaction also showed resonances attributable to Cp_2Mo (1-hexene), as well as one at δ 4.54 for an unidentified product.

Similar results were obtained with cyclohexene or 2,3-dimethyl-2-butene in place of 1-hexene; with diphenylacetylene, resonances attributable to $\text{C}_{20}\text{H}_{18}\text{Mo}_2$, unreacted Cp_2MoO , and some Cp_2MoH_2 were observed, as well as one at δ 4.28 (s) attributable to the $\text{Cp}_2\text{Mo}(\text{PhC}\equiv\text{CPh})$ complex.

Irradiation of Cp_2MoO under a CO Atmosphere. A solution of Cp_2MoO (40 mg, 0.16 mmol) in benzene or pyridine saturated with CO gas was irradiated ($\lambda > 340$ nm; 1 h in pyridine or 4 h in benzene). Following filtration, an infrared spectrum of the supernatant solution showed a band in the CO stretching region corresponding to Cp_2MoCO : pyridine, 1907 cm^{-1} ; benzene, 1915 cm^{-1} .¹²

Irradiation of Cp_2MoO in SEt_2 . A solution of 30 mg (0.12 mmol) of Cp_2MoO in SEt_2 (4 mL) was freeze-pump-thaw-degassed (three cycles) and then irradiated ($\lambda > 490$ nm) for 3 h. The solution changed color from green to yellow-brown, and a brown precipitate deposited. The $^1\text{H NMR}$ spectrum (in benzene- d_6 after evaporation of the solvent) showed resonances due to the dehydromolybdocene dimer (7%), $\text{Cp}_2\text{Mo}(\text{H})\text{SR}$ (10%), and a trace amount of Cp_2MoH_2 . Some of the chemical shifts of $\text{Cp}_2\text{Mo}(\text{H})\text{SR}$ were at δ -7.38 (s, Mo-H) and 4.46 (s, Cp H). There were resonances at δ 3.71 (s), 3.80 (s), 3.80 (s), 3.89 (s), 3.94 (s), 4.03 (s) (all assigned to the Cp of Cp_2MoL), and 6.00–7.00 (broad multiplet; assigned to L of Cp_2MoL where L = unsaturated organic products). There were additional resonances around δ 1.6–2.5 (m), 2.95 (br), 3.5 (m), 4.18 (s), 4.21 (s), 4.25 (s), 4.66 (s), and 4.67 (s) that could not be assigned unambiguously.

Synthesis of $\text{Cp}_2\text{Mo}(\text{H})\text{SEt}$. THF (20 mL) was added to a mixture of $\text{Cp}_2\text{Mo}(\text{SEt})_2$ (0.2 g, 0.57 mmol) and Cp_2MoH_2 (0.12 g, 0.53 mmol). (Some of the $\text{Cp}_2\text{Mo}(\text{SEt})_2$ remained undissolved.) After 48 h the color of the mixture changed from brown to orange-brown. The solvent was evaporated, the residue was extracted with benzene (4×20 mL), and the resulting solution was placed on a 30×2 cm alumina column (made with the alkaline alumina described above and with hexane). Elution with benzene removed unreacted Cp_2MoH_2 , which eluted first as a yellow solution. Changing to a 1/10 THF/benzene solvent mixture produced an orange band. Slow evaporation of the solvent gave flaky, light orange crystals of $\text{Cp}_2\text{Mo}(\text{H})\text{SEt}$ (72%). Anal. Calc for $\text{C}_{12}\text{H}_{16}\text{SMo}$: C, 50.00; H, 5.60; S, 11.12. Found: C, 49.97; H, 5.42; S, 11.25. $^1\text{H NMR}$ (benzene- d_6): δ 4.44 (d, $J_{\text{Cp-H}} = 1.4$ Hz, 10 H, Cp), 2.25 (q, $J_{1,2} = 6.2$ Hz, 2.4 H, $-\text{S}-\text{CH}_2$), 1.43 (t, $J = 7.3$ Hz, 3.8 H, CH_3), -7.37 (s, 0.9 H, Mo-H). IR (Nujol): 1830 cm^{-1} , $\nu(\text{Mo}-\text{H})$.

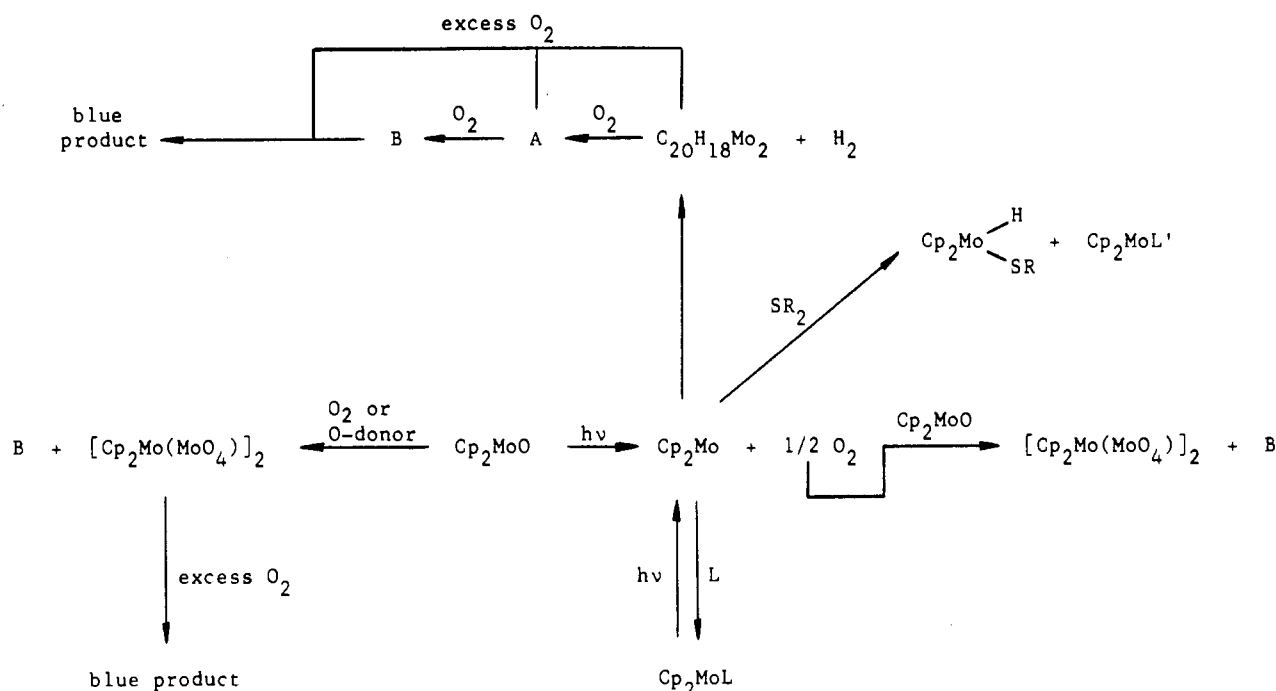
Synthesis of $\text{Cp}_2\text{Mo}(\text{H})\text{SCH}_3$. The same procedure as above was followed, using 30 mg (0.13 mmol) of Cp_2MoH_2 and 0.1 g (0.31 mmol) of $\text{Cp}_2\text{Mo}(\text{SMe})_2$ in 15 mL of THF. As with $\text{Cp}_2\text{Mo}(\text{SEt})_2$, not all of the $\text{Cp}_2\text{Mo}(\text{SMe})_2$ dissolved. After workup and slow evaporation of the solvent, an orange solid was obtained (38 mg). $^1\text{H NMR}$ (benzene- d_6): δ 4.45 (d, $J_{\text{Cp-H}} = 1.4$ Hz, 10 H, Cp), 2.02 (s, 3 H, CH_3), -7.35 (s, 1 H, Mo-H). Anal. Calc for $\text{C}_{11}\text{H}_{14}\text{SMo}$: C, 48.18; H, 5.14; S, 11.69. Found: C, 48.19; H, 5.19; S, 12.31. IR (Nujol): 1840 cm^{-1} , $\nu(\text{Mo}-\text{H})$.

Calculations. Calculations were carried out by the SCF- $X\alpha$ -SW method.¹³⁻¹⁷ Overlapping spheres were used. Schwarz's α_{HF} values were

- (7) Heller, H. G.; Langan, J. R. *J. Chem. Soc., Perkin Trans. 2* **1981**, 341–343.
 (8) deMayo, P.; Shizuka, H. In *Creation and Detection of the Excited State*; Ware, W. R., Ed.; Dekker: New York, 1976; Vol. 4, pp 139–215.
 (9) (a) Fischer, E. O.; Hristidu, Y. Z. *Naturforsch., B: Anorg. Chem., Org. Chem.* **1960**, *15B*, 135–136. (b) Green, M. L. H.; McCleverty, J. A.; Pratt, L.; Wilkinson, G. J. *J. Chem. Soc.* **1961**, 4854–4859. (c) King, R. B. In *Organometallic Syntheses*; Eisch, J. J., King, R. B., Eds.; Academic: London, 1965; p 79. (d) Green, M. L. H.; Knowles, P. J. J. *J. Chem. Soc., Perkin Trans. 1* **1973**, 989–991.
 (10) (a) Nakamura, A.; Otsuka, S. *J. Mol. Catal.* **1976**, *1*, 285–307. (b) Adam, G. J. S.; Green, M. L. H. *J. Organomet. Chem.* **1981**, *208*, 299–308.

- (11) Thomas, J. L. *J. Am. Chem. Soc.* **1973**, *95*, 1838–1847.
 (12) Geoffroy, G. L.; Bradley, M. G. *Inorg. Chem.* **1978**, *17*, 2410–2414.
 (13) Slater, J. C. *The Calculation of Molecular Orbitals*; Wiley: New York, 1979.
 (14) Johnson, K. H. *Adv. Quantum Chem.* **1973**, *7*, 143–185.
 (15) Rosch, N.; Klemperer, W.; Johnson, K. H. *Chem. Phys. Lett.* **1973**, *23*, 149–154.

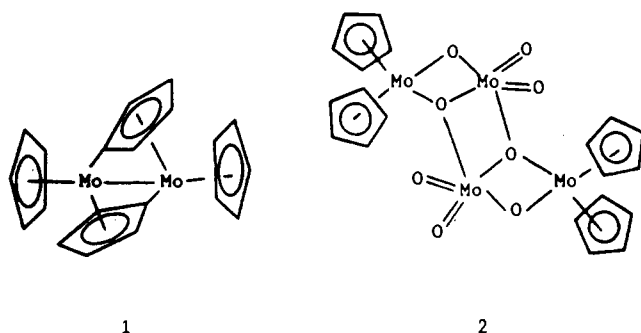
Scheme I



used for the atomic exchange parameters.^{18,19} The values for the intersphere and outer-sphere regions were a weighted average of the atomic values, where the weights are the number of valence electrons on the different neutral free atoms. A minimal basis set in partial wave expansions was used.²⁰ The Cp₂MoO structure⁴ was idealized to C_{2v} symmetry.

Results

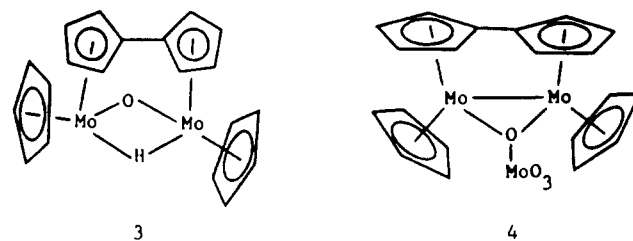
Irradiation of (C₅H₅)₂MoO in Benzene and/or Pyridine. Irradiation ($\lambda > 600$ or 300 nm) of Cp₂MoO in benzene gave rise to a very slow reaction. The main products are the dehydromolybdocene dimer²¹ $[(\eta^5\text{-C}_5\text{H}_5)_2(\mu\text{-}\eta^1, \eta^5\text{-C}_5\text{H}_4)_2\text{Mo}_2]$ (**1**), henceforth abbreviated C₂₀H₁₈Mo₂, the molybdocene molybdate dimer $[\text{Cp}_2\text{Mo}(\text{MoO}_4)]_2$ ^{10b} (**2**), and an unidentified product that



we will refer to as component A (Scheme I). Mass spectroscopic analysis of the gas above the reacted solution showed that O₂ formed in substantial amounts. For reasons to be explained shortly, the quantity of O₂ formed cannot be predicted by any simple stoichiometry. Hence, no attempt was made to quantify the amount of O₂ formed. The C₂₀H₁₈Mo₂ complex was identified by ¹H NMR spectroscopy (Table I), and $[\text{Cp}_2\text{Mo}(\text{MoO}_4)]_2$ was characterized by elemental analysis²² and infrared spectroscopy

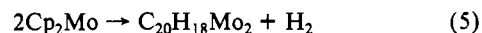
(Table I) by comparison to an authentic sample.^{10b}

Elemental analysis showed that complex A contained a substantial amount of oxygen (14.6%), in addition to carbon (41.2%) and hydrogen (3.4%). However, the data did not fit any simple formulation. Infrared spectroscopic data showed numerous absorption bands in the region 800–1070 cm⁻¹, one or more of which might be due to $\nu(\text{Mo-O})$ (Table I). The proton NMR spectrum has a pattern that is similar to but not identical with that of C₂₀H₁₈Mo₂ and complex 3 (Table I).²³ Another possible for-

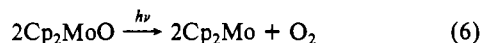


mulation, $\{[\text{Mo}(\eta^5\text{-C}_5\text{H}_5)_2(\mu\text{-OMoO}_3)(\mu\text{-}\eta^5\text{-C}_5\text{H}_4\text{-}\eta^5\text{-C}_5\text{H}_4)]\}$ (**4**), seems unlikely since this complex is sparingly soluble in DMSO whereas complex A is quite soluble in this solvent.²³

The dehydromolybdocene (C₂₀H₁₈Mo₂) dimer is known to form by dimerization of two Cp₂Mo fragments:²¹



The reactivity of the Cp₂MoO complex thus suggests that the photochemistry of this species is described by the following process:



Further support for this reaction comes from reactions whose details are given below. In addition, the reactions leading to $[\text{Cp}_2\text{Mo}(\text{MoO}_4)]_2$ and complex A are described later.

Irradiation ($\lambda > 300$ nm) of Cp₂MoO in pyridine led to a much faster reaction than in benzene to give the same products as above. Typically, the reaction was completed in 3 h instead of 24–48 h. No pyridine *N*-oxide was detected by IR or ¹H NMR spectroscopy.²⁴ Qualitatively, we observed that when the reaction was

- (16) Johnson, K. H.; Smith, F. C. *Phys. Rev. B* **1972**, *5*, 831–843.
 (17) Bruce, M. R. M.; Kenter, A.; Tyler, D. R. *J. Am. Chem. Soc.* **1984**, *106*, 639–644.
 (18) Schwarz, K. *Phys. Rev. B* **1972**, *5*, 2466–2468.
 (19) Schwarz, K. *Theor. Chim. Acta* **1974**, *34*, 225–231.
 (20) Weber, J.; Geoffroy, M.; Goursoit, A.; Penigault, E. *J. Am. Chem. Soc.* **1978**, *100*, 3995–4003.
 (21) Green, M. L. H.; Berry, M.; Cooper, N. J.; Simpson, S. J. *J. Chem. Soc., Dalton Trans.* **1980**, 29–39.

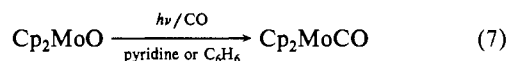
- (22) Anal. Calc for C₂₀H₂₀O₈Mo₄: C, 31.09; H, 2.59; O, 16.58. Found: C, 32.14; H, 2.86; O, 17.39.
 (23) Baskin, J.; Green, M. L. H.; Poveda, M. L.; Prout, K. *J. Chem. Soc., Dalton Trans.* **1982**, 2485–2495.

Table II. ^1H NMR Chemical Shift Data for the Cp Resonances in Cp_2MoL (L = Phosphorus Ligand)

L	chem shift, δ	solvent
PPh_3	3.90 ($J_{\text{P-H}} = 4.4$ Hz)	C_6D_6
PPh_3	3.69 ($J_{\text{P-H}} = 4.6$ Hz)	$\text{DMSO}-d_6$
PPh_3	3.88 ($J_{\text{P-H}} = 4.4$ Hz)	$\text{C}_6\text{D}_6/\text{py}-d_5$
$\text{P}(n\text{-Bu})_3$	3.96 ($J_{\text{P-H}} = 4.2$ Hz)	C_6D_6
$\text{P}(n\text{-Bu})_3$	3.97 ($J_{\text{P-H}} = 4.2$ Hz)	$\text{C}_6\text{D}_6/\text{py}-d_5$
$\text{P}(O\text{-}n\text{-Bu})_3$	4.21 ($J_{\text{P-H}} = 4.8$ Hz)	$\text{C}_6\text{D}_6/\text{py}-d_5$
$\text{P}(\text{OEt})_3$	4.19 ($J_{\text{P-H}} = 4.8$ Hz)	C_6D_6
$\text{P}(\text{OEt})_3$	4.17 ($J_{\text{P-H}} = 4.8$ Hz)	$\text{C}_6\text{D}_6/\text{py}-d_5$
$\text{P}(\text{OPh})_3$	4.10 ($J_{\text{P-H}} = 5.2$ Hz)	$\text{C}_6\text{D}_6/\text{py}-d_5$

run in a mixture of pyridine and benzene, the rate depended on the solvent ratio, with the rate increasing as the concentration of pyridine increased.

It was possible to trap the molybdocene formed in the reactions above by irradiating Cp_2MoO in the presence of CO:

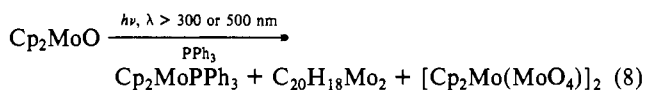


The adduct Cp_2MoCO was identified by infrared spectroscopy [$\nu(\text{C}\equiv\text{O})$: 1907 cm^{-1} in pyridine; 1915 cm^{-1} in benzene].¹² Apart from the formation of much brown precipitate (see Experimental Section), no other product was detected in these reactions. Formation of the Cp_2MoCO adduct provides further support for the premise that reaction 6 occurs.

Irradiation of Cp_2MoO in DMSO or CH_3CN . Irradiation ($\lambda > 340\text{ nm}$) of Cp_2MoO in DMSO led to the slow formation of 1 and 2; A was not detected. The NMR spectrum of the reaction solution showed two broad resonances in the region 6.4–6.7 ppm due to an unidentified product, B. This product was also formed whenever Cp_2MoO or $\text{C}_{20}\text{H}_{18}\text{Mo}_2$ was exposed to O_2 . Irradiation of Cp_2MoO ($\lambda > 500\text{ nm}$) in acetonitrile gave the same result as above except that a small amount of A was also detected.

Irradiation of Cp_2MoO and Amines. Irradiation ($\lambda > 360\text{ nm}$) of Cp_2MoO and quinuclidine, NEt_3 , or NEt_2H in benzene or pyridine led only to the same products as in benzene or pyridine alone. No amine *N*-oxides were detected by ^1H NMR or infrared spectroscopy. Reactions with *n*- BuNH_2 or 1-methylimidazole also gave no oxygenated products.

Irradiation of Cp_2MoO and Phosphines. Irradiation ($\lambda > 300$ or 500 nm) of Cp_2MoO in benzene in the presence of an excess of PPh_3 led to the products in eq 8. The products were char-



acterized by ^1H NMR spectroscopy (Table IV), but no Ph_3PO was detected. The absence of Ph_3PO was also confirmed by infrared spectroscopy [$\nu(\text{P}=\text{O})$: 1204 cm^{-1} in C_6H_6].²⁵ A control (dark) sample reacted only slightly (<1% in the same time, 9 h; 25°C) to give the same products as in the photochemical reaction.

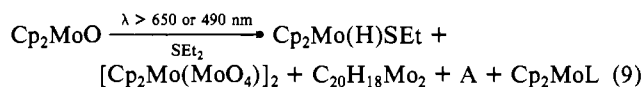
The reaction above was repeated a number of times, and in several instances, small amounts of Ph_3PO were formed, as detected by ^1H NMR spectroscopy. The molecular oxygen formed in the photolysis may be reacting photochemically with PPh_3 to form Ph_3PO .²⁵

Cp_2MoO was also irradiated in the presence of other phosphines. In most cases, substantial amounts of Cp_2MoPR_3 were detected by ^1H NMR spectroscopy (Table II). However, irradiation of Cp_2MoO in the presence of $\text{P}(\text{C}_6\text{H}_{11})_3$ gave only $\text{C}_{20}\text{H}_{18}\text{Mo}_2$ and $[\text{Cp}_2\text{Mo}(\text{MoO}_4)]_2$. The inability to form $\text{Cp}_2\text{MoP}(\text{C}_6\text{H}_{11})_3$ was probably due to steric crowding.²⁶

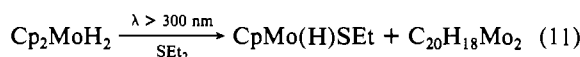
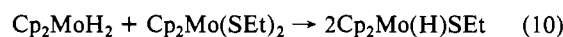
Irradiation of Cp_2MoO and Unsaturated Hydrocarbons. Irradiation ($\lambda > 300\text{ nm}$ or 600 nm) of Cp_2MoO in the presence of

cyclohexene, 1-hexene, or diphenylacetylene gave $\text{C}_{20}\text{H}_{18}\text{Mo}_2$ and a brown precipitate (the usual mixture of $[\text{Cp}_2\text{Mo}(\text{MoO}_4)]_2$ and complex A) as major products. Small amounts of Cp_2MoL (L = unsaturated hydrocarbon) were also detected by ^1H NMR spectroscopy (see Experimental Section).¹¹ With cyclohexene or 1-hexene, the dark reactions gave larger amounts of Cp_2MoL than the photochemical reactions, probably because the Cp_2MoL species are photosensitive. No epoxides were detected.

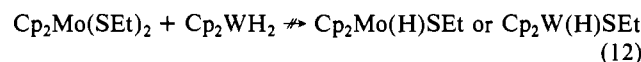
Visible Irradiation of Cp_2MoO and SEt_2 . Irradiation ($\lambda > 650$ or 490 nm) of Cp_2MoO and SEt_2 gave the products indicated in reaction 9. Complex A was identified by IR and ^1H NMR



spectroscopy, and $[\text{Cp}_2\text{Mo}(\text{MoO}_4)]_2$ and $\text{C}_{20}\text{H}_{18}\text{Mo}_2$ were identified by IR and ^1H NMR spectroscopy, respectively. The $\text{Cp}_2\text{Mo}(\text{H})\text{SEt}$ complex was identified as a product by comparison of its NMR spectrum to the spectrum of authentic $\text{Cp}_2\text{Mo}(\text{H})\text{SEt}$. The latter spectrum was obtained by synthesizing this new complex by two alternate routes:



In each reaction, formulation of the product as $\text{Cp}_2\text{Mo}(\text{H})\text{SEt}$ was consistent with elemental analysis, infrared spectroscopy, and ^1H NMR data (Table I). Note that reaction 12 did not occur.

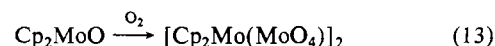


Visible irradiation ($\lambda > 490$ or 650 nm) of Cp_2MoO in SMe_2 did not give any $\text{Cp}_2\text{Mo}(\text{H})\text{Me}$; the only products were $\text{C}_{20}\text{H}_{18}\text{Mo}_2$, complex A, and $[\text{Cp}_2\text{Mo}(\text{MoO}_4)]_2$.

It is interesting to speculate on the mechanism of $\text{Cp}_2\text{Mo}(\text{H})\text{SEt}$ formation in reaction 9. Reaction 11 suggests that Cp_2Mo is an intermediate, as irradiation of Cp_2MoH_2 is known to yield Cp_2Mo .¹² Oxidative addition of SR_2 to Cp_2Mo , followed by β -hydrogen elimination, would yield the product. [Cp_2Mo also reacts to form $\text{C}_{20}\text{H}_{18}\text{Mo}_2$ (eq 5), another of the products in eq 9.] The inability of Cp_2MoO to react ($\lambda > 490\text{ nm}$) with SMe_2 to yield $\text{Cp}_2\text{Mo}(\text{H})\text{Me}$ is consistent with a β -elimination pathway.

The species Cp_2MoL formed in reaction 9 were not fully characterized. They exhibited up to seven proton NMR signals in the region 3.60–4.20 ppm that are attributable to cyclopentadienyl protons. Cp resonances in this region are typical of Cp_2MoL -type complexes (see Table II for example), where L is a neutral ligand.¹¹ The presence of so many Cp resonances suggests there are a number of complexes corresponding to different L's, and the presence of accompanying resonance signals suggests that L may be an olefinic species that is formed through fragmentation of a thioether. For example, the unsaturated species may be formed by β -hydrogen elimination as outlined above. Irradiation ($\lambda > 300\text{ nm}$) of a solution containing the species tentatively formulated as Cp_2MoL led to the disappearance of all the proton NMR signals that are assigned to these species and to the formation of $\text{C}_{20}\text{H}_{18}\text{Mo}_2$. Irradiation of Cp_2MoL complexes is known to yield $\text{C}_{20}\text{H}_{18}\text{Mo}_2$,³¹ consistent with our formulation of the Cp_2MoL product in reaction 9. This result also shows that Cp_2MoL is not an intermediate in the formation of $\text{Cp}_2\text{Mo}(\text{H})\text{SEt}$.

Reaction of Cp_2MoO with O_2 . The reaction of Cp_2MoO with traces of O_2 in benzene solution gave a brown precipitate that was found to be predominantly $[\text{Cp}_2\text{Mo}(\text{MoO}_4)]_2$, as determined by infrared spectroscopy (Table III).



The same product formed when Cp_2MoO was reacted with an excess of O_2 except that complex B also formed. Prolonged exposure of these products to air yielded an unidentified blue precipitate. Both the blue species and $[\text{Cp}_2\text{Mo}(\text{MoO}_4)]_2$ are insoluble in all common organic solvents.

(24) The spectra of the reaction solutions were compared to the spectrum of authentic pyridine *N*-oxide obtained from Aldrich.

(25) Geoffroy, G. L.; Denton, D. A.; Eigenbrot, C. W., Jr. *Inorg. Chem.* **1976**, *15*, 2310–2311.

(26) Tolman, C. A. *Chem. Rev.* **1977**, *77*, 313–348.

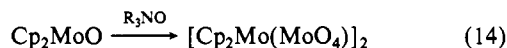
Table III. Quantum Yields for the Disappearance of (RC₅H₄)₂MoO (R = H, CH₃)

oxide	[Cp ₂ Mo], M	medium	absorbed intens., ×10 ⁹ einsteins/s	irradiation wavelength, nm	quantum yield
Cp ₂ MoO	1.0 × 10 ⁻²	py	3.7	436	0.25
Cp ₂ MoO	1.5 × 10 ⁻²	py	3.8	436	0.91
Cp ₂ MoO	2.0 × 10 ⁻²	py	3.8	436	3.1
Cp ₂ MoO	3.1 × 10 ⁻³	<i>n</i> -BuNH ₂	4.4	436	0.21 ± 0.06
(MeCp) ₂ MoO	2.8 × 10 ⁻³	<i>n</i> -BuNH ₂	2.9	436	0.040 ± 0.013
(MeCp) ₂ MoO	4.3 × 10 ⁻³	<i>n</i> -BuNH ₂	3.2	436	0.072 ± 0.008
(MeCp) ₂ MoO	9.8 × 10 ⁻³	<i>n</i> -BuNH ₂	4.4	436	0.10 ± 0.01
(MeCp) ₂ MoO	4.6 × 10 ⁻³	<i>n</i> -BuNH ₂	9.3	546	0.061 ± 0.007
(MeCp) ₂ MoO	8.1 × 10 ⁻³	py	4.6	436	0.057
(MeCp) ₂ MoO	7.9 × 10 ⁻³	py/PPh ₃ (0.2 M)	4.6	436	0.053
(MeCp) ₂ MoO	4.3 × 10 ⁻³	1-methylimidazole	3.5	436	0.047 ± 0.008
(MeCp) ₂ MoO	9.2 × 10 ⁻³	1-methylimidazole	3.5	436	0.11 ± 0.03
(MeCp) ₂ MoO	6.7 × 10 ⁻³	C ₆ H ₆	4.3	436	4.8 × 10 ⁻³
(MeCp) ₂ MoO	6.5 × 10 ⁻³	C ₆ H ₆ /PPh ₃ (0.2 M)	4.3	436	5.2 × 10 ⁻³

Table IV. Selected SCF-X α -SW Molecular Orbitals for Cp₂MoO

orbital	energy, eV	occupation no. (no. of electrons)	% charge distribution			major contributing atomic orbital(s)
			Mo	C(Cp)	O	
11b ₂	-2.18	0	60	17	8	d(Mo) + p(Cp)
6a ₂	-2.48	0	50	14	0	d(Mo) + p(Cp)
8b ₁	-3.45	0	50	0	18	d(Mo) + p(O)
13a ₁	-5.32	2	56	6	3	d(Mo)
10b ₂	-5.49	2	6	22	19	p(Cp) + p(O)
7b ₁	-6.54	2	9	17	4	p(Cp) + d(Mo)
12a ₁	-6.81	2	22	25	4	p(Cp) + d(Mo)
5a ₂	-7.60	2	37	8	0	d(Mo) + p(Cp)
9b ₂	-9.26	2	3	58	6	p(Cp)
6b ₁	-9.62	2	23	2	55	p(O) + d(Mo)
8b ₂	-9.67	2	23	12	47	p(O) + d(Mo)
10a ₁	-11.29	2	28	14	54	p(O) + d(Mo)
4a ₁	-23.37	2	15	1	79	s(O) + d(Mo)

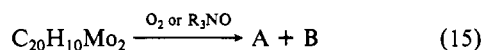
Cp₂MoO also reacted with Me₃NO and *N*-methylmorpholine *N*-oxide in benzene to give [Cp₂Mo(MoO₄)] as the major product as shown in reaction 14. These reactions were complete in



R₃NO = Me₃NO, *N*-methylmorpholine *N*-oxide

seconds. The same reaction was observed with CH₃NO₂, although the reaction required ~5 min. The reactions with pyridine *N*-oxides were even slower (~1 h).

Reaction of C₂₀H₁₈Mo₂ with Oxygen Donors. C₂₀H₁₈Mo₂ reacted with O₂ and other oxygen donors at room temperature to yield species A and B (eq 15). In a typical experiment, 15 mg



R₃NO =

Me₃NO, 4-picoline *N*-oxide, *N*-methylmorpholine *N*-oxide

of C₂₀H₁₈Mo₂ reacted with 10 mg of 4-picoline *N*-oxide in benzene to yield 7 mg of A.

Quantum Yields. The quantum yields for various reactions are listed in Table III. These quantum yields are not necessarily indicative of the photochemical efficiency because oxygen (one of the products) reacts with the starting material. However, these data (especially with brief irradiation times) may still be used qualitatively to explain certain reactivity patterns. Thus, Table III shows a number of trends, among which are the following. (1) The quantum yields increased as the concentration of the metallocene oxide increased. This is especially evident for the first three entries in Table III. (2) The quantum yields increased with donor ability of the medium. For example, the quantum yields in pyridine, *n*-BuNH₂, and 1-methylimidazole are much higher than those obtained in benzene. Also, the polarity (or dielectric constant, ϵ) of aprotic media does not seem to affect the quantum yields. Thus, although no quantum yields were measured, it was qualitatively observed that reactions were much faster in pyridine ($\epsilon = 12$), dimethyl sulfide ($\epsilon \approx 4$), or *n*-BuNH₂

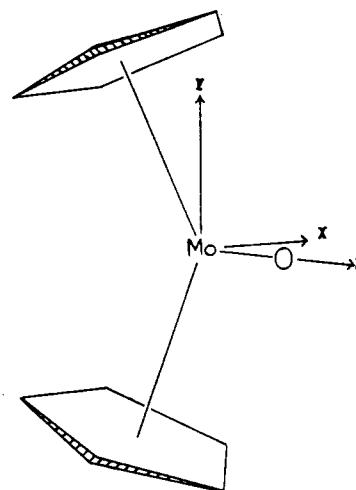


Figure 1. Coordinate system used in the SCF-X α -SW molecular orbital calculation.

($\epsilon \approx 10$) than in acetone ($\epsilon = 20$), acetonitrile ($\epsilon = 37$), or DMSO ($\epsilon = 45$). (3) The reactivity decreased on moving from Cp₂MoO to (MeCp)₂MoO. Finally, recall that the photochemistry is qualitatively the same at all wavelengths; i.e., the same products form with either high- or low-energy radiation.

Electronic Structure of the Cp₂MoO Complex. In order to interpret the optical and photochemical properties of the Cp₂MoO molecule better, an SCF-X α -SW molecular orbital calculation was carried out on the complex.¹³ Figure 1 shows the coordinate system used for the calculation, and the results are summarized in Table IV. These results are more easily interpreted when viewed as part of the molecular orbital energy diagram shown in Figure 2. Depicted in this figure are the interactions of oxo ligand orbitals with the frontier orbitals of a bent Cp₂Mo²⁺ fragment.²⁷

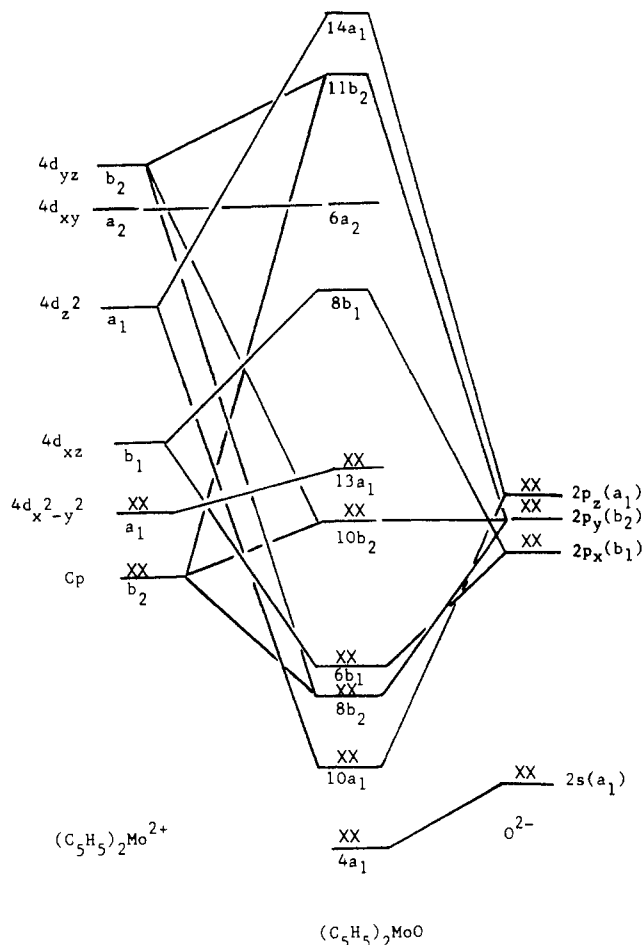


Figure 2. Qualitative molecular orbital energy diagram of the Cp_2MoO complex showing principal orbital interactions for selected orbitals. The diagram is qualitative and not drawn to scale. The descriptions of the d orbitals in the $\text{Cp}_2\text{Mo}^{2+}$ fragment are qualitative; see ref 27 for a more complete analysis of these orbital compositions.

(Molecular orbitals that are not relevant to this discussion were not included in Figure 2.)

The oxo ligand has three orbitals available for bonding to the bent $\text{Cp}_2\text{Mo}^{2+}$ fragment: $2p_z(a_1)$, $2p_x(b_1)$, and $2p_y(b_2)$. (The $2s(a_1)$ orbital of the oxo ligand is so low in energy that it essentially does not participate in bonding to $\text{Cp}_2\text{Mo}^{2+}$.²⁸) These orbitals interact with the $4d_{z^2}(a_1)$, $4d_{xz}(b_1)$, and $4d_{yz}(b_2)$ orbitals to form a σ bond [$2p_z/4d_{z^2}$ (bonding = $10a_1$, antibonding = $14a_1$)] and two π bonds [$2p_x/4d_{xz}$ (bonding = $6b_1$, antibonding = $8b_1$) and $2p_y/4d_{yz}$ (bonding = $8b_2$, antibonding = $10b_2$ and $11b_2$)], as shown in Figures 2 and 3. The Mo–O bond order is less than 3, however, because the (filled) $10b_2$ orbital is Mo–O π , antibonding (Figure 3c). This filled Mo–O antibonding orbital arises because the $4d_{yz}$ orbital also interacts with a filled SALC orbital of b_2 symmetry on the cyclopentadienyl ligands. The situation is thus one in which one acceptor orbital (the Mo $4d_{yz}$) interacts with two donor orbitals (the Cp b_2 and O $2p_y$ orbitals), giving rise to one unfilled and two filled molecular orbitals. [From symmetry considerations and the data in Table IV, these molecular orbitals are $8b_2$ (Mo–O bonding), $10b_2$ (a mixture of Cp and oxygen; Mo–O antibonding), and $11b_2$ (mostly Mo with some Cp; Mo–Cp and Mo–O antibonding).] The apportionment of the Mo, Cp, and O basis orbitals among these three molecular orbitals is such that the $10b_2$ orbital is slightly Mo–O π , antibonding. Hence, the Mo–O bond order is expected to be between 2 and 3; indeed, the Mo–O bond distance⁵ (1.721 Å in $(\text{MeCp})_2\text{MoO}$) and the Mo–O stretching frequencies^{4,5} in Cp_2MoO (800 cm^{-1}) and $(\text{MeCp})_2\text{MoO}$ (827

Table V. Selected Calculated Electronic Transitions in Cp_2MoO

transition	allowed or forbidden	transition type	qual description	transition wavelength, nm
$13a_1 \rightarrow 8b_1$	allowed	d–d	$d_{x^2-y^2} \rightarrow d_{zz}$	686
$10b_2 \rightarrow 8b_1$	forbidden	LMCT	Cp, O $\rightarrow d_{zz}$	617
$13a_1 \rightarrow 6a_2$	forbidden	d–d	$d_{x^2-y^2} \rightarrow d_{xy}$	426
$10b_2 \rightarrow 6a_2$	allowed	LMCT	Cp, O $\rightarrow d_{xy}$	398
$7b_1 \rightarrow 8b_1$	allowed	LMCT	Mo–Cp $\rightarrow d_{zz}$	398
$13a_1 \rightarrow 11b_2$	allowed	d–d	$d_{x^2-y^2} \rightarrow d_{yz}$	393
$10b_2 \rightarrow 11b_2$	allowed	LMCT	Cp, O $\rightarrow d_{yz}$	374
$12a_1 \rightarrow 8b_1$	allowed	LMCT	Mo–Cp $\rightarrow d_{zz}$	363
$6b_1 \rightarrow 8b_1$	allowed	LMCT	Mo–O(π^*) \rightarrow (d_{zz})	200

Table VI. Electronic Spectra of the $(\text{RC}_5\text{H}_4)_2\text{MoO}$ Complexes (R = H, CH_3)

R	solvent	λ , nm (ϵ)
CH_3	CH_2Cl_2	683, 422 (sh), 398
H	C_6H_6	653, 430 (sh)
CH_3	C_6H_6	672, 435, 380 (sh)
H	C_6H_{12}	635
H	THF	650
CH_3	THF	672, 425 (sh), 375 (sh)
H	py	656 (170), 430 (sh)
CH_3	py	678, 425 (sh)
H	CH_3CN	661, 453
CH_3	CH_3CN	682, 435 (sh), 380 (sh)
CH_3	<i>i</i> -PrOH	702, 428 (sh), 390
CH_3	CH_3OH	700
H	DMF	665, 396
$(\text{C}_5\text{H}_5)_2\text{WO}$	THF	530 (190), 385

cm^{-1}) suggest the presence of not much more than a Mo–O double bond.^{5,29}

The bonding situation described above (i.e. having more donor electron pairs available than acceptor orbitals) is not unusual in complexes with π -donor ligands. A typical example is found with the $\text{Mn}(\text{CO})_5\text{I}$ complex: the iodide ligand is a π donor (as well as a σ donor), yet the only acceptor orbitals available for the π electrons are also acceptor orbitals for σ electrons. As is always the case in this situation, the π donation shows up as a mixing of the acceptor and two (or more) donor orbitals in the molecular orbital wave function.

To complete this discussion of Figures 2 and 3, note that, as expected, a d orbital [the $d_{x^2-y^2}(13a_1)$] is the highest occupied molecular orbital.

In previous $X\alpha$ calculations on organometallic systems, we demonstrated that the relative energies of electronic transitions can be adequately approximated by taking the differences in orbital energies.^{17,30} The predicted electronic transitions in the Cp_2MoO complex and their corresponding energies are listed in Table V. The lowest energy allowed absorption band is expected to arise from the $13a_1 \rightarrow 8b_1$ transition, which is best characterized as a d–d transition. The next allowed absorption band is predicted to be a ligand-to-metal charge-transfer (LMCT) transition, $10b_2 \rightarrow 6a_2$, involving both the cyclopentadienyl and oxo ligands. Other calculated transitions are indicated in Table V. These may be compared to the electronic spectra reported in Table VI; there is good agreement between the observed and calculated transition energies. The electronic spectra are discussed in more detail in the next section.

It is important to note that the $8b_1$ and $11b_2$ molecular orbitals are antibonding (π^*) with respect to the Mo–O bond and the $11b_2$ is also antibonding with respect to the Mo–Cp bond. Similarly, $6a_2$ is antibonding with respect to the Mo–Cp bond. Therefore, both d–d and LMCT transitions may lead to metal–Cp and/or metal–O bond weakening while enhancing the electrophilicity of the ligands.

(28) Brindley, P. B.; Davies, A. G.; Hawari, J. J. *Organomet. Chem.* **1983**, *250*, 247–256.

(29) Stiefel, E. I. In *Progress in Inorganic Chemistry*; Lippard, S. J., Ed.; Wiley: New York, 1977; Vol. 22, pp 1–223.

(30) Bruce, M. R. M.; Bruce, A. E.; Tyler, D. R. *Polyhedron* **1985**, *4*, 2073–2081.

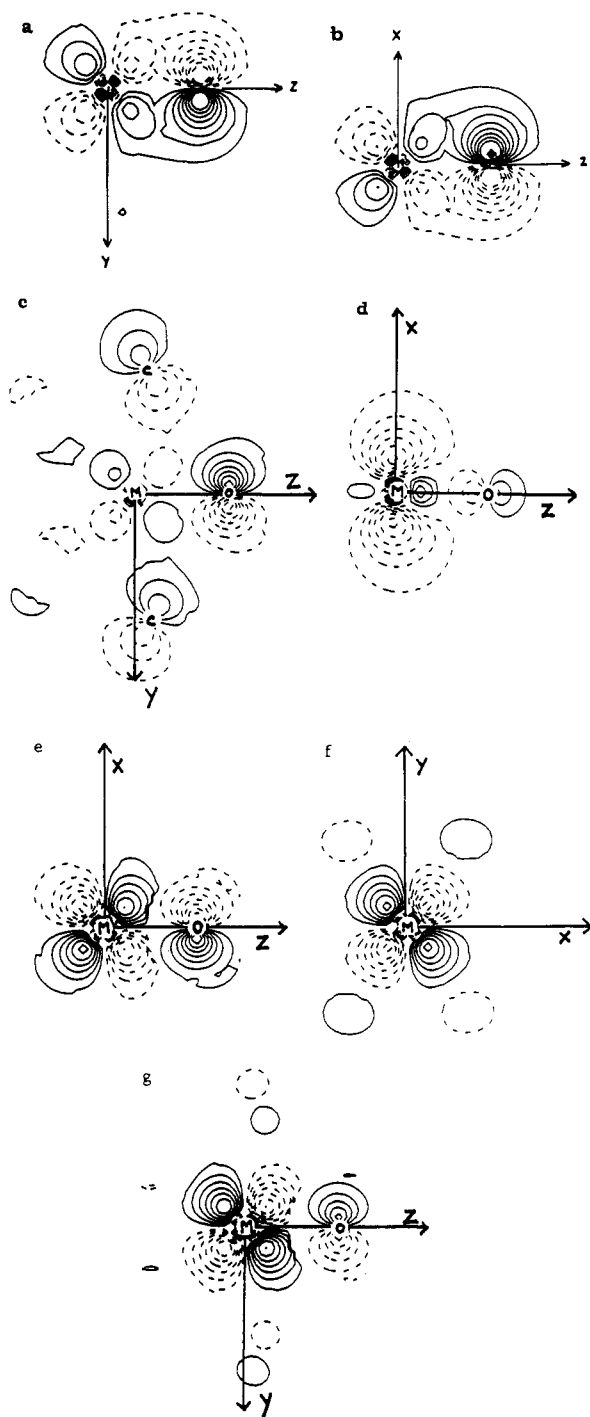


Figure 3. Wave function contour plots for Cp₂MoO: (a) 8b₂, yz plane; (b) 6b₁, xz plane; (c) 10b₂, yz plane; (d) 13a₁, xz plane; (e) 8b₁, xz plane; (f) 6a₂, xy plane; (g) 11b₂, yz plane. See Figure 1 for coordinate system. Solid lines denote contours at values of 0.05–0.40 e^{1/2} bohr^{-3/2}, while broken lines denote values of –0.05 to –0.40 e^{1/2} bohr^{-3/2}.

Electronic Spectra of (RC₅H₄)₂MO (M = Mo; R = H, CH₃).

The electronic spectra of these complexes have three major features in the region $\lambda > 250$ nm (Table VI). First, there is an absorption band with λ_{\max} in the region 650–700 nm ($\epsilon \sim 150$ –200 M⁻¹ cm⁻¹). This band is the lowest energy feature in all of the spectra, and therefore it is assigned to the metal-centered 13a₁ → 8b₁ (d–d) transition, the lowest energy transition predicted by the calculation. The band is red-shifted on moving from Cp₂MoO to (MeCp)₂MoO as it is when the medium becomes more polar and/or acidic.

The second feature is two relatively weak peaks ($\epsilon \sim 50$ –100 M⁻¹ cm⁻¹) that overlap to form a broad unsymmetrical band in the 350–450-nm region. It is difficult to correlate the position of this band with changes in the nature of the solvent because the band overlaps with a very intense absorption at shorter wavelength.

The feature, however, is more pronounced in (MeCp)₂MoO, where the very intense UV band is more blue-shifted than in Cp₂MoO. It is also more pronounced in hydroxylic solvents (e.g. 2-propanol) or very polar solvents (e.g. DMF). The calculation suggests that the composite band may be due to several of many transitions: 13a₁ → 11b₂ (d–d), 10b₂ → 6a₂ (Cp, O → Mo), 10b₂ → 11b₂ (Cp, O → Mo), 7b₁ → 8b₁ (Cp → Mo), 12a₁ → 8b₁ (Cp → Mo).

The third feature is a very intense band ($\epsilon \geq 5000$ M⁻¹ cm⁻¹) that extends from the UV region ($\lambda_{\max} < 250$ nm) with a tail trailing into the visible region. This band is blue-shifted as the medium becomes more polar as it is for (MeCp)₂MoO compared to Cp₂MoO. This band probably arises from ligand-to-metal charge-transfer (LMCT) transitions involving oxygen and/or Cp. For example, the transition(s) might be 12a₁ → 8b₁ (calc $\lambda = 363$ nm; Cp → Mo), 12a₁ → 11b₂ (calc $\lambda = 267$ nm; Cp → Mo), or 6b₁ → 8b₁ (calc $\lambda = 200$ nm; O → Mo).

Discussion

Cp₂MoO was irradiated in the presence of phosphines, amines, olefins, and sulfides with the intent of transferring an oxygen atom to these molecules. In the case of amines, olefins, and sulfides, no oxygenated products were formed under any conditions. Under certain conditions with PPh₃, small amounts of OPPh₃ were formed. However, oxygen is a photoproduct of the irradiation of Cp₂MoO, and it is well-known that O₂ reacts photochemically with PPh₃ in the presence of metal complexes to yield OPPh₃.²⁵ Thus, it was not possible to determine the mechanism of OPPh₃ formation. Nevertheless, it is reasonable to conclude that Cp₂MoO is a poor photochemical oxygenating agent. This conclusion holds regardless of whether the excitation is at low energy (into a d–d band) or at high energy (into an OMCT band).

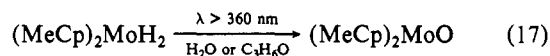
The descriptive photochemistry of the Cp₂MoO complex, Scheme I, can be interpreted in terms of the following initial reaction:



An important point to emphasize is that reaction 16 occurs in nonpolar, noncoordinating solvents as well as in polar, coordinating solvents. The reaction is more efficient, however, in coordinating solvents (Table III). The formation of molecular oxygen in reaction 16 was established by mass spectroscopy, and the intermediate formation of Cp₂Mo is suggested by the nature of the products that result from the photolysis. Specifically, the formation of C₂₀H₁₈Mo₂ implies the intermediacy of Cp₂Mo because the former is known to result from dimerization of the latter (eq 5).²¹ In addition, Cp₂Mo could be intercepted with ligands (eq 7 and 8).

The generation of O₂ has consequences for the overall reactivity of the Cp₂MoO/h ν system because the C₂₀H₁₈Mo₂ product and Cp₂MoO itself are oxygen sensitive. Thus, C₂₀H₁₈Mo₂ reacts with O₂ or other oxygenating agents (e.g. ONR₃) to yield complex A. Further reaction of complex A with O₂ yields B and eventually a blue precipitate. The blue precipitate was not characterized, but it is probably a mixture of molybdates. Cp₂MoO reacts with O₂ (or oxygenating agents) to yield [Cp₂Mo(MoO₄)₂], complex B, and eventually the blue precipitate.

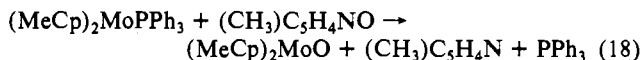
Results from several other experiments give insights into the reason that Cp₂MoO cannot be used as a photochemical oxygenating agent. Thus, irradiation of (MeCp)₂MoH₂ in the presence of H₂O or propylene oxide gave (MeCp)₂MoO (74% and 16% yields, respectively):



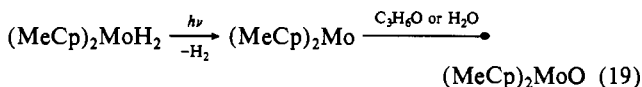
These reactions are similar to those reported by Green and co-workers, who obtained Cp₂WO by irradiating Cp₂WH₂ in the presence of propylene oxide.³¹ (Green also reported obtaining Cp₂MoO by reducing Cp₂MoCl₂ with sodium amalgam in the presence of propylene oxide.³¹) In a similar experiment, we also

(31) Berry, M.; Davies, S. G.; Green, M. L. H. *J. Chem. Soc., Chem. Commun.* 1978, 99–100.

observed that addition of 4-picoline *N*-oxide to $(\text{MeCp})_2\text{MoPPh}_3$ gave $(\text{MeCp})_2\text{MoO}$:



On the basis of the known photochemistry of Cp_2MoH_2 , it is reasonable to propose that reaction 17 occurs by initial photolytic formation of Cp_2Mo followed by oxygen atom transfer:



The intermediate $(\text{MeCp})_2\text{Mo}$ is also undoubtedly involved in reaction 18. Clearly, these reactions establish that Cp_2Mo (or $(\text{MeCp})_2\text{Mo}$) is a better oxygen atom acceptor than an alkene or an amine, and it is for this reason that no net photochemical oxygenation reactions occur with the Cp_2MoO complex. Even if O atom transfer were occurring, $\text{C}_{20}\text{H}_{18}\text{Mo}_2$ (the product of Cp_2Mo coupling) and Cp_2MoO are reactive toward O atom donors (eq 14 and 15), and it is unlikely that oxygenated substrates would be stable in the presence of these species. The most reasonable conclusion to draw from this study, therefore, is that no *net* oxygen atom transfer to the substrates results from irradiation of the Cp_2MoO complex.

Conclusions. The initial reaction in the photochemistry of Cp_2MoO is the formation of Cp_2Mo and O_2 (eq 16). Most of the observed products arise from the reaction of O_2 with Cp_2MoO and the products derived from Cp_2Mo .

Net oxygen atom transfer from the excited state of Cp_2MoO to nucleophiles in anhydrous and oxygen-free media does not occur because Cp_2Mo , Cp_2MoO , and $\text{C}_{20}\text{H}_{18}\text{Mo}_2$ are generally better oxygen atom acceptors than the nucleophiles.

The photochemistry of the Cp_2MoO complex is qualitatively independent of excitation wavelength, and it is likely, therefore, that the lowest energy excited state (d-d) gives rise to the reactivity and not an LMCT excited state. As eq 16 implies, the formation of O_2 from Cp_2MoO is a bimolecular process, and hence LMCT excitation is not necessarily required for O_2 formation. In a subsequent paper, we will report on our characterization of the bimolecular intermediate formed when Cp_2MoO is irradiated in solution at -78°C .

Acknowledgment. This work was supported by a University Exploratory Research Grant from Procter and Gamble Co. D.R.T. acknowledges the Sloan Foundation for a fellowship. Professors W. Klemperer and Jim Mayer are thanked for helpful discussions.

Registry No. 1, 66705-66-6; 2, 78356-94-2; Cp_2MoO , 37298-36-5; Cp_2MoH_2 , 1291-40-3; $(\text{MeCp})_2\text{MoH}_2$, 61112-91-2; $(\text{MeCp})_2\text{MoO}$, 98525-67-8; $\text{Cp}_2\text{Mo}(1\text{-hexene})$, 117095-12-2; Cp_2MoCO , 12701-85-8; Et_2S , 352-93-2; $\text{Cp}_2\text{Mo}(\text{H})\text{SEt}$, 117095-13-3; $\text{Cp}_2\text{Mo}(\text{SEt})_2$, 37328-23-7; $\text{Cp}_2\text{Mo}(\text{H})\text{SCH}_3$, 117095-14-4; $\text{Cp}_2\text{Mo}(\text{SMe})_2$, 83136-50-9; O_2 , 7782-44-7; $\text{Cp}_2\text{MoPPh}_3$, 63672-64-0; Cp_2WH_2 , 1271-33-6; $(\text{MeCp})_2\text{MoPPh}_3$, 117095-19-9; $\text{Cp}_2\text{MoP}(n\text{-Bu})_3$, 117095-15-5; $\text{Cp}_2\text{MoP}(O\text{-}n\text{-Bu})_3$, 117095-16-6; $\text{Cp}_2\text{MoP}(\text{OEt})_3$, 117095-17-7; $\text{Cp}_2\text{MoP}(\text{OPh})_3$, 117095-18-8; 1-hexene, 592-41-6; cyclohexene, 110-83-8; 2,3-dimethyl-2-butene, 563-79-1; diphenylacetylene, 501-65-5.